UDC 544.723.214+544.72.023.2+549.521.4+54-31+546.26.-162

CHEMICAL DESIGN OF CARBON-COATED Al_2O_3 NANOPARTICLES

L.F. Sharanda*, I.V. Babich, Yu.V. Plyuto

Chuiko Institute of Surface Chemistry of National Academy of Sciences of Ukraine
17 General Naumov Street, Kyiv 03164, Ukraine

The novel approach to chemical design of carbon-coated Al_2O_3 nanoparticles with an average particle size of 8-10 nm was developed. Carbon coating was synthesised by modification of fumed alumina support with 4,4'-methylenebis-(phenylisocyanate) and its subsequent pyrolysis at 700°C. In order to synthesise the samples with increased carbon content, the grafting-pyrolysis cycle was repeated. The above mentioned synthetic route resulted in the samples with carbon loading of 7.6 and 14.5 wt. %. Characterisation of the synthesised samples with Raman, FTIR, TG/DTG-DTA, N_2 adsorption and SEM techniques revealed the formation of continuous carbon coating on the surface of Al_2O_3 nanoparticles after the first grafting-pyrolysis cycle. The increase of the carbon loading on the alumina surface to 14.5 wt. % (two grafting-pyrolysis cycles) resulted in the formation of the carbon coating with more regular graphitic structure.

INTRODUCTION

The carbon films have attracted considerable attention due to their unique properties including chemical and mechanical stability, electrical conductivity, optical transparency, and low friction coefficient. Combination of physicochemical properties of individual carbon and alumina in carbon-coated alumina results in novel materials promising for the development of dense electrically conductive ceramic [1] and fillers [2], membranes [3], solar absorbers [4], catalyst supports and catalysts [5], protective coating [6]. It is well established that the properties, structures and uniformity of carbon film and the degree of surface coverage of the support strongly depend on the preparation conditions, carbon source, deposition parameters and the supports chemical nature [1–6]. Therefore, a number of approaches for the synthesis of such carbon-coated materials has been reported.

The first approach proposed by Youtsey et al. [2] and intensively used by Leboda et al. [7] is based on the ability of organic compounds to be pyrolysed on the surface of the alumina and silica-alumina supports at elevated temperatures that is accompanied by carbon deposition. Among the tested organic substances pyrolysable in the range of 600–700°C, are such hydrocarbons as hexane, benzene, toluene, naphthalene, anthracene, cyclohexane and cyclohehene which was found to be the most promising for making carbon-alumina and carbon-silica-alumina composite materials. Pyrolysis of organic alcohols like *n*-heptyl and benzyl proceeds at lower temperatures [8].

An alternative approach was developed by Pratsinis et al. [9] who proposed a continuous, one-step flame-synthesis of carbon-coated titania and silica nanostructured particles. The diffusion flame aerosol reactor is used for simultaneous combustion of organic and inorganic sources. In both one-step methods the formation of separate carbon phase along the carbon coating cannot be completely excluded because of the applied synthesis conditions.

The present work aims at the development of two-step approach for the synthesis of carbon-coated nanoparticles. It is based on chemical grafting of 4,4'-methylenebis(phenylisocyanate) (MDI) on the support surface and subsequent pyrolysis of the resulting surface species in vacuum. The method was demonstrated for chemical design of carbon-coated Al_2O_3 nanoparticles whose detailed physicochemical characterisation was performed.

EXPERIMENTAL

Non-porous fumed alumina ($S_{BET}(N_2)$=155 m^2g^{-1}) with an average particle size of 5–8 nm, prepared by the hydrolysis of aluminium chloride in a hydrogen/oxygen flame, was used as the alumina support. MDI was obtained from Bayer AG and used without further purification. The weighted amount (4.5 g) of fumed alumina was contacted with 100 ml of 0.04 M *o*-xylene solution of MDI at room temperature for 24 h at periodic stirring. The product

* Corresponding author *lyusharanda@yahoo.com*

was filtered, washed out with 200 ml of pure *o*-xylene, dried at 60°C for 2 h. Then, the sample was placed into a quartz cell and evacuated at 700°C and a pressure of $1 \cdot 10^{-2}$ Pa for 2 h in order to complete pyrolysis of the grafted MDI. To prepare the samples with increased carbon content, the grafting-pyrolysis cycle was repeated. The above procedure resulted in samples with carbon content of 7.6 and 14.5 wt. % denoted hereafter as $C(7.6)/Al_2O_3$ and $C(14.5)/Al_2O_3$, respectively.

The Raman spectra were performed by an automated double spectrometer DFC-24 (LOMO, Russia) using excitation of Ar ion laser at λ=514.5 nm.

FTIR spectra in a reflectance mode were recorded in the range from 4000 to 400 cm^{-1} with a spectral resolution of 8 cm^{-1} using a Nexus Nicolet FTIR spectrometer (Thermo Scientific) equipped with a Smart Collector reflectance accessory. Alumina samples were powdered with KBr in 1:10 ratio.

Thermal studies (TG/DTG-DTA) were carried out with a STA-1500 H thermobalance (PL Thermal Sciences) at a heating rate of 10°C/min in an air flow of ~50 cm^3/min. The carbon content in the synthesised samples was determined gravimetrically from the weight loss within the temperature interval of 300–700°C.

The surface area (BET) and porosity were determined by nitrogen adsorption/desorption at -196°C using a Quantachrome Autosorb-6B equipment. The samples were preliminary heated in vacuum at 150°C for 16 h.

X-ray diffraction (XRD) patterns were recorded in the range 5–80° (scanning step 0.1°) with a DRON-3M automated diffractometer using the Cu-K_α (λ=1.54178Å) radiation and Ni filter.

SEM images were obtained with a LEO 1550 high resolution electron microscope. An electron beam of 2.5 kV was used to analyse the surface details of the samples.

RESULTS AND DISCUSSION

4,4'-methylenebis(phenylisocyanate) was selected as carbon precursor because of extraordinary reactivity of −N=C=O groups and high carbon content. It is well know that addition of organic isocyanates to the compounds containing mobile hydrogen atom (i.e. water, amines, carboxylic acids, alcohols) leads to urethane or urea group generation [10, 11]. The high reactivity of isocyanates toward nucleophilic reagents is mainly connected with electrophilic character of the carbon atom in −N=C=O functional group [10, 11]. Thus, the formation of surface complexes of 4,4'-methylenebis(phenylisocyanate) on the alumina surface should be expected due interaction of carbon atom of isocyanate group and oxygen atom of hydroxyl group of the alumina support that results in simultaneous transfer of the proton to the nitrogen atom. The reaction between the hydroxyl group of the alumina surface and isocyanate group can be illustrated as follows (Fig. 1).

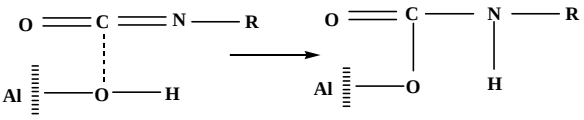

Fig. 1. Schematic representation of the reaction of −N=C=O groups of MDI with OH groups of Al_2O_3 nanoparticles

Upon the contact of Al_2O_3 nanoparticles with MDI dissolved in *o*-xylene, their initial white colour immediately turned yellow that is accompanied by discoloration of the solution. The resulting MDI species appeared to be strongly bound to the support surface since the modified Al_2O_3 nanoparticles do not loose yellow colour even after washing with *o*-xylene. This confirms that the reaction of −N=C=O groups of MDI with OH groups at the alumina surface results in the formation of the surface organic moiety.

Fig. 2 shows the SEM images of the initial fumed Al_2O_3 nanoparticles in comparison with Al_2O_3 nanoparticles whose surface was involved into interaction with 4,4'-methylenebis(phenylisocyanate).

In the SEM image of the initial fumed alumina one can see the individual Al_2O_3 nanoparticles with an average particle size of 5–8 nm and also their agglomerates with a size about 50–100 nm (Fig. 2*a*). The morphology of Al_2O_3 nanoparticles after interaction with 4,4'-methylenebis(phenylisocyanate) differs significantly (Fig. 2*b*) from that of the initial fumed alumina. One can clearly see the distinct boundaries between Al_2O_3 nanoparticles. This can indicate that surface MDI species at the alumina surface cover each individual Al_2O_3 nanoparticle that results in their separation from one another.

FTIR spectroscopy proves the chemical interaction of isocyanate group (−N=C=O) of MDI with OH groups of Al_2O_3 nanoparticles.

First, in FTIR spectrum of MDI (Fig. 3*a*), a distinct absorption band at 2278 cm^{-1} typical for isocyanate group (−N=C=O) is observed [12]. This band is not present in the spectrum of the alumina sample which contacted with MDI (Fig. 3*b*). Instead, one can see the intensive broad bands centred at 3520 and 3340 cm^{-1} which correspond to free and hydrogen bonded N−H groups, respectively [13].

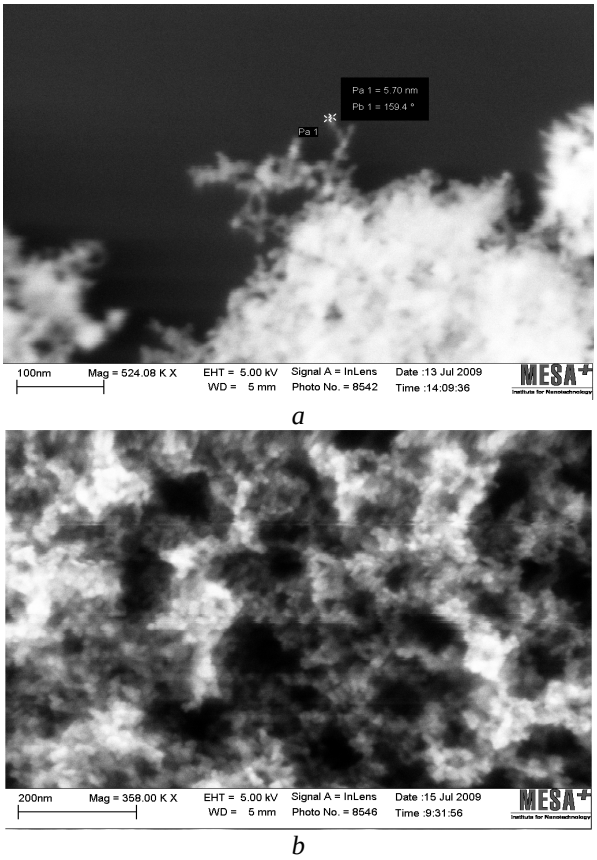

Fig. 2. *a* – SEM images of the initial Al_2O_3 nanoparticles; *b* – after their interaction with 4,4'-methylenebis(phenylisocyanate)

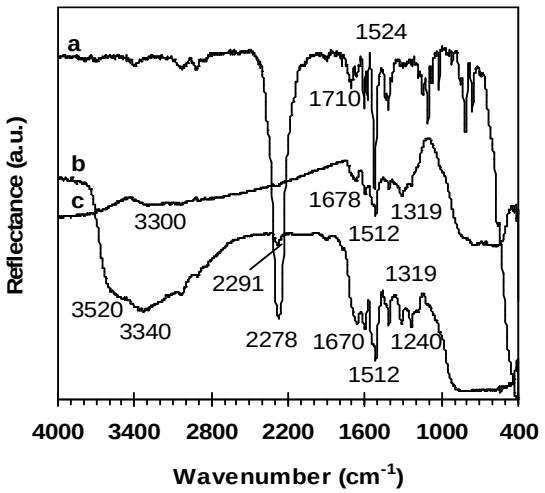

Fig. 3. *a* – FTIR spectra of individual MDI, *b* – MDI on the surface of Al_2O_3 nanoparticles *c* – C(7.6)/Al_2O_3 sample

Second, when MDI interacts with the alumina surface, the appearance of the new absorption band at 1670 cm^{-1} and the shoulder around 1545 cm^{-1} which can be assigned to so-called Amide I and Amide II vibrations in amide groups −NH−C(O)− is observed (Fig. 3*b*). Besides, the new absorption bands at 1319 cm^{-1} which is due to (N−H) + (C−N) stretching vibrations and at 1240 cm^{-1} attributed to the C−N stretching vibrations of amide group appeared [12, 14]. This also confirms the formation of surface MDI species according to Fig. 1.

Besides, the formation of surface MDI species can also proceed via interaction of −N=C=O groups with coordinatively unsaturated Al^{3+} acid sites on the alumina surface. It has been found earlier [15] that −N=C=O groups posses very strong electron-donor property and may be used to identify even very weak Lewis acid sites of the alumina surface.

One can also see that the band at 2278 cm^{-1} associated with −N=C=O groups is not present in the spectrum of the carbon-coated alumina sample which contacted with MDI (Fig. 3*c*). In addition, the bands at 1678 and 1545 cm^{-1} which indicate the formation of the amide bonds (NH−CO) is observed. This allowed us to conclude that the carbon-coated alumina possesses the surface functional groups which can be involved into strong interaction with MDI molecules.

It is necessary to note the difference between MDI grafting on the initial and carbon-coated Al_2O_3 nanoparticles. In contrast to MDI grafted on the surface of Al_2O_3 nanoparticles (Fig. 3*b*), in FTIR spectrum of MDI on the surface of C(7.6)/Al_2O_3 sample (Fig. 3*c*) only a weak broad band centered at 3300 cm^{-1} connected with hydrogen-bonded N−H groups is seen. Moreover, the band which can be assigned to free N−H groups is not present at all. This reflects substantial changes of the nature of the adsorption sites due to shielding of the alumina surface with the deposited carbon.

The surface loading of Al_2O_3 nanoparticles with MDI species and carbon coating was determined by thermal analysis using TG/DTG-DTA technique (Table 1).

Table 1. Quantitative data on MDI grafting on Al_2O_3 nanoparticles, carbon yield upon pyrolysis of surface MDI species and carbon loading

Sample	Carbon loading, wt. %	Grafted MDI, wt. %	Pyrolysis of grafted MDI		S_{BET} (N_2), m^2/g
			yield of elemental carbon, %	final carbon loading, wt. %	
Al_2O_3	0	19.2	55.0	7.6	155.0
C(7.6)/Al_2O_3	7.6	12.8	75.0	14.5	155.0
C(14.5)/Al_2O_3	14.5	–	–	–	155.0

One can see that on the surface of Al_2O_3 nanoparticles the amount of grafted MDI reaches 19.2 wt. %. The carbon loading in this sample after pyrolysis was 7.6 wt. % that corresponds to 55% of carbon yield. The amount of MDI grafted on the $C(7.6)/Al_2O_3$ sample appeared to be somewhat lower as compared to that on the initial alumina support. Meanwhile, the carbon yield after pyrolysis was sufficiently higher (75.0%). After two-fold repetition of the grafting-pyrolysis cycle the carbon loading on the surface of Al_2O_3 nanoparticles was 14.5 wt. %.

Thermoanalytical characterisation of the synthesised carbon coated Al_2O_3 nanoparticles exhibits the intense weight loss in DTG patterns around 500°C that coincides with the exothermic peak in DTA curves. Oxidation started at 300°C and proceeded in one step up to 700°C. This suggests that oxidation of a single carbon phase occurs.

The nitrogen adsorption-desorption isotherms confirmed that carbon coating did not change the textural characteristics of Al_2O_3 nanoparticles (see Fig. 4).

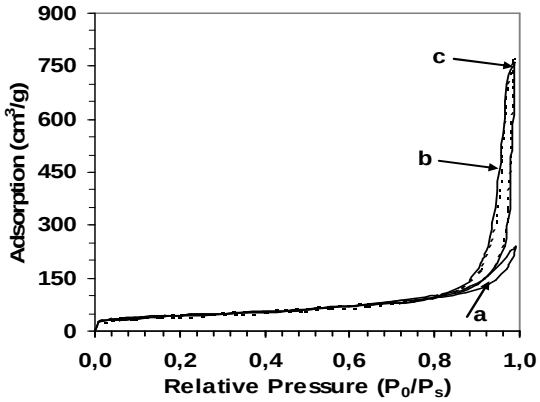

Fig. 4. Nitrogen adsorption-desorption isotherms on Al2O3 nanoparticles – *a*, C(7.6)/Al2O3 – *b* and C(14.5)/Al2O3 – *c* samples

The nitrogen adsorption-desorption isotherms of the initial Al_2O_3 nanoparticles and carbon-coated samples (Fig. 4) can be identified as the type II isotherms according to IUPAC classification and are typical for non-porous materials [16]. The surface area values of the initial and carbon-coated Al_2O_3 nanoparticles are similar as well (see Table 1). This means that the structure and particles size of the initial fumed Al_2O_3 nanoparticles were not changed upon carbon deposition. The difference is observed only in the region near saturation pressure of the volume adsorption for both $C(7.6)/Al_2O_3$ and $C(14.5)/Al_2O_3$ samples where adsorption appeared to be increased significantly in comparison with the initial Al_2O_3 nanoparticles. Most likely this is due to the decrease of close packing of the primary Al_2O_3 nanoparticles when their surface is covered with carbon coating.

Raman spectroscopy was used to characterise the structure of carbon coatings on the alumina surface.

The Raman spectrum of $C(7.6)/Al_2O_3$ sample (Fig. 5*a*) consists of two bands, namely a broad asymmetric band centred at 1585 cm^{-1} which relates to sp^2-bonded carbon of mono-crystalline graphite (known as G-band) and the band at 1365 cm^{-1} which is associated with disorder in the graphite lattice (known as D-band) [17–23]. The presence of such well resolved broad Raman bands indicates the formation of the carbon coating with amorphous structure [17–19] on the surface of fumed Al_2O_3 after the first grafting-pyrolysis cycle.

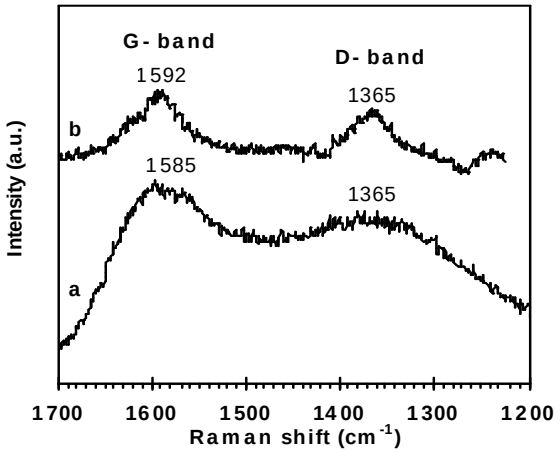

Fig. 5. Raman spectra of $C(7.6)/Al_2O_3$ – *a*, and $C(14.5)/Al_2O_3$ – *b* samples

The bandwidth and the intensity of both D- and G-bands in Raman spectrum of $C(14.5)/Al_2O_3$ sample are decreased substantially (Fig. 5*b*). This can indicate the formation of the less defective disordered graphite structure and the increase of the number and/or the size of sp^2 domains after the repetition of the grafting-pyrolysis cycle [20].

It is important to mention that the Raman spectrum of $C(14.5)/Al_2O_3$ sample appeared be very similar to that of the cathode outer shell carbon materials [24] or polycrystalline graphite produced by ball milling of the graphite powder [23]. It should be also noted that similar transformations are observed in Raman spectra of amorphous carbon films upon thermal treatment [20–24]. Usually, such transformations in carbon materials (know as graphitisation) occur at high temperatures (over 1200°C) but can also proceed at lower temperatures in the presence of catalysing agents like ceramic oxides [1]. Therefore, we suppose that

alumina surface promotes ordering of the amorphous carbon coating at lower temperature.

The analysis of FTIR spectra also suggests the existence of graphite-like carbon structure on the alumina surface (Fig. 6*a*,*b*).

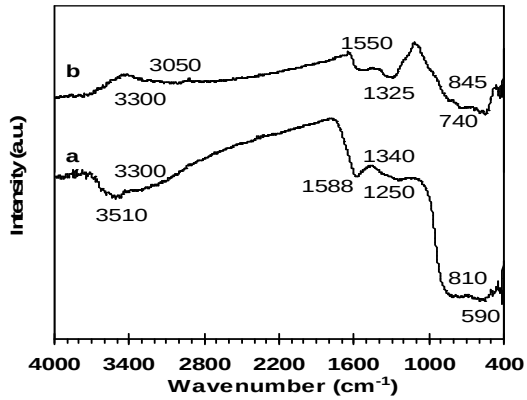

Fig. 6. FTIR spectra of C(7.6)/Al_2O_3 – *a* and C(14.5)/Al_2O_3 – *b* samples

As can be seen, the FTIR spectrum of C(7.6)/Al_2O_3 sample (Fig. 6*a*) exhibits the band at 1588 cm^{-1} which is attributed to typical aromatic ring vibrations (sp^2-C−C) [17, 23–29]. The band centered at 1250 cm^{-1} indicates the existence of defects in graphitic structure [25]. Besides, the bands centred at 1340 and 3510 cm^{-1} which can be assigned to C−N and N−H groups, respectively, are observed as well [28–30].

FTIR spectrum of C(14.5)/Al_2O_3 sample is shown in Fig. 6*b*. As one can see, repetition of the grafting-pyrolysis cycle results in substantial change of FTIR spectrum in the region of 4000–400 cm^{-1}. The band at 1588 cm^{-1} shifted to 1550 cm^{-1} and became considerably less intensive. This indicated the increase of the size of the graphitic domains in carbon coating on the alumina surface [25, 26]. Besides, the band near 1340 cm^{-1} which relates to stretching vibrations of C−N groups shifted to 1325 cm^{-1} while the band at 1250 cm^{-1} which corresponds to disordered graphite-like structure disappeared. These changes clearly indicate that the increase of the carbon loading on the alumina surface to 14.5 wt. % resulted in the formation of the carbon coating with less defective graphitic structure [25]. One can also see the bands at 740 and 845 cm^{-1} which are due to the presence of C−H groups in aromatic rings [17, 25] and/or aromatic impurities in graphite [26]. In Fig. 6*b* the band at 3510 cm^{-1} is not observed and the spectrum exhibits the presence of very weak bands centred at 3300 and 3050 cm^{-1} which can be related to C−H groups in different configuration [17, 25, 28].

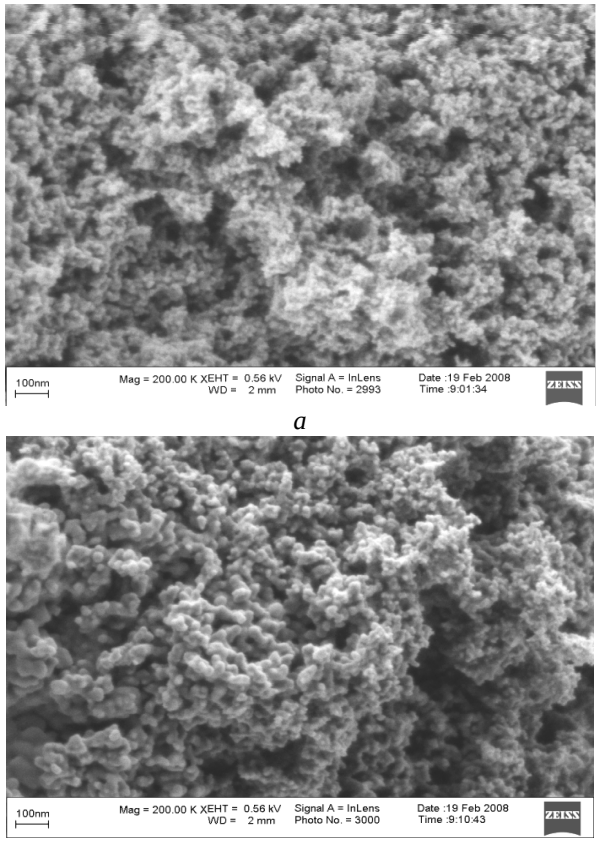

Fig. 7. SEM images of the carbon-coated C(7.6)/Al_2O_3 – *a* and C(14.5)/Al_2O_3 – *b* samples

The observed changes can indicate that population of surface functional surface groups in C(14.5)/Al_2O_3 sample is smaller in comparison with that in C(7.6)/Al_2O_3 sample. Besides, we can also come to the conclusion that the surface structure of carbon coating in C(7.6)/Al_2O_3 and C(14.5)/Al_2O_3 samples differs significantly. The carbon coating after the first grafting-pyrolysis cycle possesses the defective structure and the repetition of the grafting-pyrolysis cycles results in the formation of more uniformed and less defective carbon coating on the alumina surface.

The surface morphology of the synthesised carbon-coated Al_2O_3 nanoparticles was examined by SEM (Fig. 7).

The morphology of the carbon-coated Al_2O_3 nanoparticles (Fig. 7*a*,*b*) differs significantly from the initial Al_2O_3 nanoparticles (Fig. 2*a*). The SEM images of both C(7.6)/Al_2O_3 and C(14.5)/Al_2O_3 samples showed the spherical, non-agglomerated nanoparticles with the size of 8–10 nm that indicates the covering of the surface of individual Al_2O_3 nanoparticles with a carbon coating. Thus, the formation of continuous carbon coating on the alumina surface occurs after the first grafting-pyrolysis cycle.

CONCLUSIONS

Novel approach to chemical design of carbon-coated Al_2O_3 nanoparticles was developed. The synthesis of carbon coating on fumed Al_2O_3 nanoparticles is based on grafting of 4,4'-methylenebis (phenylisocyanate) (MDI) that proceeds via reaction of isocyanate groups (−N=C=O) with hydroxyl groups on the alumina surface and subsequent pyrolysis of surface MDI species at 700°C in vacuum. The formation of continuous carbon coating on the Al_2O_3 nanoparticles surface occurred after the first grafting-pyrolysis cycle. The increase of the carbon loading on the alumina surface to 14.5 wt. % (two grafting-pyrolysis cycles) resulted in the formation of the carbon coating with more regular graphitic structure. The SEM images of the synthesised alumina samples showed the presence of spherical, non-agglomeration carbon-coated Al_2O_3 nanoparticles with the size of 8–10 nm.

REFERENCES

1. *Menchavez R.L., Fuji M., Takahashi M*. Electrically conductive dense and porous alumina with in-situ-synthesized nanoscale carbon networks // Adv. Mater. – 2008. – V. 20, N 12. – P. 2345–2351.
2. *Pat. 4018943* United States, Method of forming a conducting material for a conducting device / K.J Youtsey et al. – Appl. No.: 05/226035; Filing: 14.02.1972; Publ.: 19.04.1977. – 8 p.
3. *Pat. 5262198* United States, Method of producing a carbon coated ceramic membrane and associated product / P.K.T. Liu et al. – Appl. No.: 07/682181; Filing: 08.04.1991; Publ.: 16.11.1993. – 11 p.
4. *Katumba G., Lu J., Olumekor L. et al.* Low cost selective solar absorber coatings: characteristics of carbon-in-silica synthesized with sol-gel technique // J. Sol-Gel Sci. Technol. – 2005. – V. 36, N 1. – P. 33–43.
5. *Zhang T., Jacobs P.D., Haynes H.W.* Laboratory evaluation of four coal liquefaction catalysts prepared from modified alumina supports // Catal. Today. – 1994. – V. 19, N 3. – P. 353–366.
6. *Mann M., Shter G.E., Grader G.S.* Preparation of carbon coated ceramic foams by pyrolysis of polyurethane // J. Mater. Sci. – 2006. – V. 41, N 18. – P. 6046–6055.
7. *Leboda R., Charmas B., Marciniak M., Skubiszewska-Zieba J.* On the topography and morphology of carbon deposits prepared by pyrolysis of alcohol on the surface of silica gel // Mater. Chem. Phys. – 1999. – V. 58, N 2. – P. 146–155.
8. *Boorman P.M., Chong K.* Preparation of carbon-covered alumina using fluorohydrocarbons. A new acidic support material // Appl. Catal. A. – 1993. – V. 95, N 2. – P. 197–210.
9. *Kammler H.K., Pratsinis S.* Carbon-coated titania nanostructured particles: continuonus, one-step flame-synthesis // J. Mater. Res. – 2003. – V. 18, N 11. – P. 2670–2676.
10. *Caraculacu A.A., Coseri S.* Isocyanates in polyaddition processes. Structure and reaction mechanisms // Prog. Polym. Sci. – 2001. – V. 26, N 5. – P. 799–851.
11. *Krol P.* Synthesis methods, chemical structures and phase structures of linear polyurethanes. Properties and applications of linear polyurethanes in polyurethane elastomers, copolymers and ionomers // Prog. Mater. Sci. – 2007. – V. 52, N 6. – P. 915–1015.
12. *Dechant J.* Ultrarotspektroskopische Untersuchungen an Polymeren / Ed. R. Danz W. Kimmer, R. Schmolke. – Akademie-Verlag-Berlin, 1972. – 347 p.
13. *Stankovich S., Piner R.D., Nguyen S.T., Ruoff R.S.* Synthesis and exfoliation of isocyanate-treated grapheme oxide nanoplatelets // Carbon. – 2006. – V. 44. – P. 3342–3347.
14. *Zhao C., Ji L., Liu H. et al.* Functionalized carbon nanotubes containing isocyanate groups // J. Solid State Chem. – 2004. – V. 177, N 12. – P. 4394–4398.
15. *Davydov A.* Molecular Spectroscopy of Oxide Catalyst Surfaces / Ed. N.T. Sheppard. – John Wiley & Sons Ltd, England, 2003. – 684 p.
16. *Gregg S.J., Sing K.S.W.*, Adsorption, Surface Area and Porosity. – London, New York: Academic Press, 1967. – 303 p.
17. *Robertson J.* Amorphous carbon // Adv. Phys. – 1986. – V. 35, N 4. – P. 317–374.
18. *Ferrari A.C., Robertson J.* Interpretation of Raman spectra of disordered and amorphous carbon // Phys. Rev. B. – 2000. – V. 61, N 20. – P. 14095–14107.
19. *Ferrari A.C.* Raman spectroscopy of grapheme and graphite: disorder, electron-phonon coupling, doping and nonadiabatic effects // Solid State Commun. – 2007. – V. 143. – P. 47–57.
20. *Theodoropoulou S., Papadimitriou D., Zoumpoulakis L., Simitzis J.* Structural and optical characterization of pyrolytic carbon derived

from novolac resin // Anal. Bioanal. Chem. – 2004. – V. 379, N 5–6. – P. 788–791.
21. *Prawer S., Rozenblum I., Orwa J.O., Adler J.* Identification of the point defects in diamond as measured by Raman spectroscopy: comparison between experiment and computation // Chem. Phys. Lett. – 2004. – V. 390, N 4–6. – P. 458–461.
22. *Takahiro K., Ookawa R., Kawatsura K. et al.* Improvement in surface roughness of nitrogen-implanted glassy carbon by hydrogen doping // Diamond Relat. Mater. – 2003. – V. 12, N 8. – P. 1362–1367.
23. *Shen T.D., Ge W.Q., Wang K.Y. et al.*. Structural disorder and phase transformation in graphite produced by ball milling // Nanostruct. Mater. – 1996. – V. 7, N 4. – P. 393–399.
24. *Eklund P.C., Holden J.M., Jishi A.* Vibrational modes of carbon nanotubes: spectroscopy and theory // Carbon – 1995. – V. 33. – P. 959–972.
25. *Ros T.G., Dillen A.J., Geus J.W, Koningsberger D.Ch.* Surface structure of untreated parallel and fishbone carbon nanofibres: an infrared study // Chem. Phys. Chem. – 2002. – V. 3, N 2. – P. 393–399.
26. *Friedel R.A., Carlson G.L.* Infrared spectra of ground graphite // J. Phys. Chem. – 1971. – V. 75, N 8. – P. 1149–1151.
27. *Rodil S.E., Muhl S., Masa S., Ferrari A.C.* Optical gap in carbon nitride films // Thin Solid Films. – 2003. – V. 433, N 1–2. – P. 119–125.
28. *Rusop M., Omer A.M.M., Adhikari S. et al.* Effect of annealing temperature on the optical, bonding, structural and electrical properties of nitrogenated amorphous carbon thin films grown by surface wave microwave plasma chemical vapor deposition // J. Mater. Sci. – 2006. – V. 41, N 2. – P. 537–547.
29. *Vasilets V.N., Hirose A., Yang Q. et al.* Characterization of doped diamond-like carbon films deposited by hot wire plasma sputtering of graphite // Appl. Phys. A. – 2004. – V. 79, N 8. – P. 2079–2084.
30. *Yang L., May P.W, Vin L. et al.* Ultra fine carbon nitride nanocrystals synthesized by laser ablation in liquid solution // J. Nanopart. Res. – 2007. – V. 9, N 6. – P. 1181–1185.

Received 07.07.2010, accepted 17.08.2010

Хімічний дизайн вуглецевого покриття на поверхні наночастинок Al_2O_3

Л.Ф. Шаранда, І.В. Бабіч, Ю.В. Плюто

Інститут хімії поверхні ім. О.О. Чуйка Національної академії наук України
вул. Генерала Наумова 17, Київ 03164, Україна, lyusharanda@yahoo.com

Розроблений новий метод хімічного дизайну вуглецевого покриття на поверхні наночастинок пірогенного Al_2O_3 розміром 8–10 нм. Вуглецеве покриття синтезували шляхом модифікування поверхні пірогенного оксиду алюмінію 4,4-метилендифенілдиізоціанатом та подальшим його піролізом при 700°С. З метою одержання зразків з більш високим вмістом вуглецю цикл "модифікування–піроліз" повторювали. Вищеописана процедура дозволила синтезувати зразки з вмістом вуглецю 7,6 та 14,5 % ваг. Дослідження синтезованих зразків методами раманівської та ІЧ-спектроскопії, ТГ/ДТГ-ДТА, низькотемпературної адсорбції азоту та СЕМ показало, що утворення суцільного вуглецевого покриття на поверхні пірогенного Al_2O_3 відбувається вже після проведення першого циклу "модифікування–піроліз". Повторення циклу "модифікування–піроліз" МДІ приводить до формування вуглецевого покриття з більш впорядкованою графітовою структурою.

Химический дизайн углеродного покрытия на поверхности наночастиц AI_2O_3

Л.Ф. Шаранда, И.В. Бабич, Ю.В. Плюто

Институт химии поверхности им. А.А. Чуйко Национальной академии наук Украины
ул. Генерала Наумова 17, Киев 03164, Украина, lyusharanda@yahoo.com

Разработан новый метод химического дизайна углеродного покрытия на поверхности наночастиц пирогенного Al_2O_3 размером 8–10 нм. Углеродное покрытие было синтезировано путем модифицирования поверхности пирогенного оксида алюминия 4,4–метилендифенилдиизоцианатом с последующим его пиролизом при 700°С. Для того чтобы синтезировать образцы с более высоким содержанием углерода, цикл "модифицирование–пиролиз" повторяли. Описанная выше процедура позволила синтезировать образцы с содержанием углерода 7,6 и 14,5% вес. Исследование синтезированных образцов методами рамановской и ИК-спектроскопии, ТГ/ДТГ-ДТА, низкотемпературной адсорбции азота и СЭМ показало, что образование сплошного углеродного покрытия на поверхности пирогенного Al_2O_3 происходит уже после проведения первого цикла "модифицирование–пиролиз". Повторение цикла "модифицирование–пиролиз" МДИ приводит к формированию углеродного покрытия с более упорядоченной графитовой структурой.